Advanced MIPAS Level 2 Data Analysis (AMIL2DA)

Project EVG1-CT-1999-00015

Report on the Characterisation of NLTE effects in MIPAS data (WPs 5510-13) (Deliverables D59, D60, D61, D62)

Manuel López-Puertas[1], Sergio Gil-López[1], Bernd Funke[1], Thomas von Clarmann[2], Norbert Glatthor[2], Sylvia Kellmann[2], Mathias Milz[2], Tilman Steck[2], Gabriele P. Stiller[2], Anu Dudhia[3], Vivienne Payne[3], Victoria Jay[4], Jolyon Reburn[4], Heinrich Bovensmann[5], Astrid Bracher[5]

[1]Instituto de Astrofisica de Andalucia, Granada, Spain

[2] Institut für Meteorologie und Klimaforschung, Universität Karlsruhe, Germany

[3] Atmospheric, Oceanic and Planetary Physics, Oxford University, United Kingdom

[4]Rutherford Appleton Laboratory Chilton, Didcot, United Kingdom

[5]Institut für Umweltphysik Universität Bremen, Germany

July 4, 2003

1 Introduction

We describe in this report a characterisation of NLTE (non-local thermodynamics equilibrium) effects in MIPAS spectra and their effects on the retrieved species proposed in the project, mainly concentrated in the MIPAS operational products, i.e. the key species pressure-temperature, O_3, CH_4, H_2O, N_2O and HNO_3 at altitudes between 10 and 60 km. It was also our objective to assess if systematic residuals unexplained in the retrieval intercomparison could be caused by NLTE emissions in the atmosphere.

We proposed to achieve these objectives by performing three different tasks:

1. By calculating LTE and NLTE MIPAS spectra with the retrieved quantities, calculating the difference spectra, and comparing and correlating them with the best-fit retrieval residuals (WP 5511).

2. As in the previous point but with the species abundances (only for O_3 and NO_2) measured (simultaneously and in the same geolocation) by NLTE free instruments as GOMOS and SCIAMACHY (WP 5512).

3. By comparing daytime and nighttime MIPAS measured spectra and characterising the differences to elucidate potential bias caused by NLTE emissions. These might also be present in the retrieval residuals and hence could help in understanding the differences between the different processors (WP 5513).

In the project, however, we have used a superior method for assessing the NLTE effects in the retrieved species, which is to perform the retrieval in LTE and in NLTE and comparing the differences. This method was not proposed in the project because of the complexity in developing a NLTE retrieval scheme, not available when the project started. In addition we have also performed an analysis of the residuals and have correlated them with the NLTE–LTE difference spectra. The NLTE and LTE retrievals were also performed for the MIPAS data correlated with

those taken by GOMOS and SCIAMACHY. By comparing both LTE and NLTE MIPAS data with independent 'NLTE free' measurements of GOMOS and SCIAMACHY we could elucidate if potential differences can be attributed to NLTE. We discuss each of these analysis in the following sections.

2 WP 5511: Effects of NLTE on MIPAS retrieved species

2.1 NLTE analysis of residuals spectra

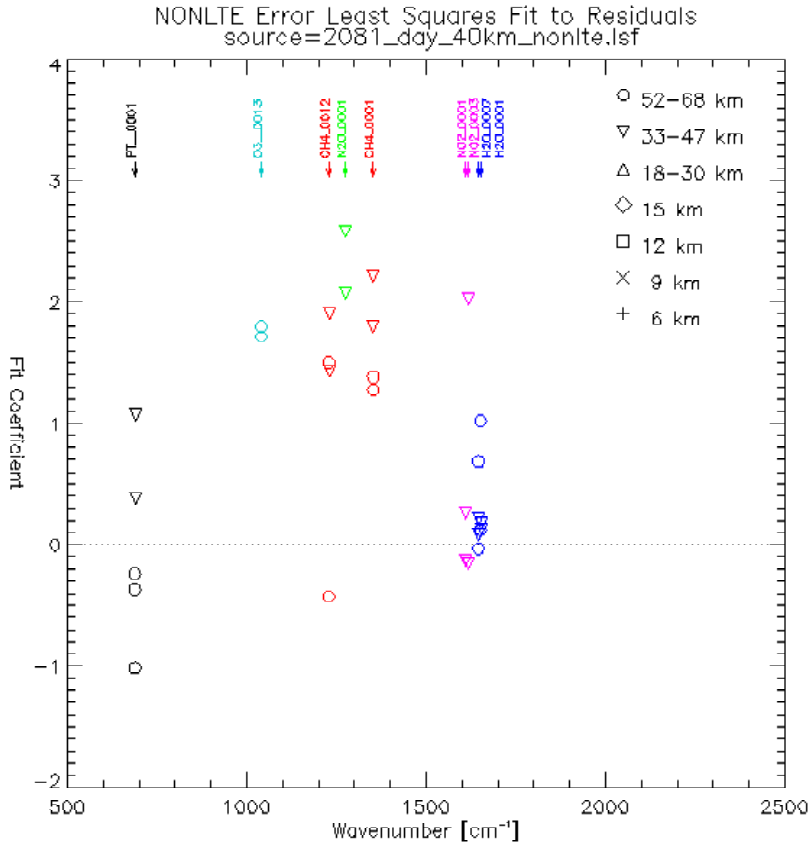

Figure 1: Residual error correlation (REC) analysis for the daytime scans of orbit 2081 (24 July 2002) at altitudes above 40 km (only open circles and inverted triangles are shown). Values are in units where +1 is the predicted (expected) sign/magnitude of the NLTE residual.

One aspect of checking the NLTE effects in the retrieved products is to analyse the residual spectra (difference between the measured spectra and the adjusted spectra resulting in the retrieval). A way of analysing it quantitatively and statistically is to correlate these residuals with the NLTE residuals, obtained as the difference between the synthetic NLTE and LTE spectra computed for an *a priori* atmosphere. This, however, give us an estimation of the upper limit effect of NLTE, since with this method NLTE cannot generally be discriminated from other error sources such as spectroscopic data (strengths) or temperature. We have analysed the residuals in the microwindows used for the retrievals at the tangent heights where they are used (occupation matrix). The analysis was done separately for day and night residuals, since NLTE in some bands is expected to be significantly dependent on illumination conditions, and also for different latitudes (6 latitude bands) and tangent heights only above 42 km. Three periods of data were analysed corresponding to July, August 2002 and orbits 2081–2083 taken also in July 2002 (the latter even corresponding to July 2002 too, were also taken because they have been extensively studied).

The results are shown in Fig. 1. In general, NLTE residuals are of similar magnitude than those predicted. NLTE in the pressure-temperature retrieval is slightly smaller than anticipated. We believe this is due to the lower collisional rate of $CO_2(v_2)$ by atomic oxygen used in the NLTE climatology. Using a faster rate, as atmospheric radiance measurements suggest (we should note that, on the contrary, laboratory data indicates values lower than that used in the climatology), drives the population of the $CO_2(v_2)$ levels to be closer to LTE, as this analysis

suggests.

NLTE effects in O_3 and H_2O are of similar magnitude to those predicted.

The effects of NLTE in CH_4 seems to be larger than those predicted by about a factor of 2. No evidence of NLTE on CH_4 has so far been reported in the literature. The NLTE populations used in selection of microwindows (López-Puertas et al., 2002) were computed using a CH_4 NLTE model with similar processes as for H_2O. It seems that the model underestimates these effects significantly. Further work on the characterisation of NLTE in CH_4, in particular by using the upper atmospheric data, is clearly needed. In consequence, potential differences in the CH_4 values retrieved by the processors including NLTE at heights above about 50 km might be explained by NLTE effects.

NLTE in N_2O is larger than predicted. However the contribution of NLTE to the N_2O total error budget is very small. Hence NLTE in N_2O is not strong enough to explain potential differences between the processors.

The effects of NLTE in NO_2 is smaller than anticipated, which is in consonance with the results of the retrievals of NO_2 NLTE parameters (see Section 2.2 below).

In summary, the analysis of NLTE from the residuals spectra suggests than NLTE is, in general, in accordance with predictions except for two cases, the NO_2 just mentioned above, for which NLTE is much smaller than anticipated, and for CH_4, which seems to be larger than predicted by a factor of 2.

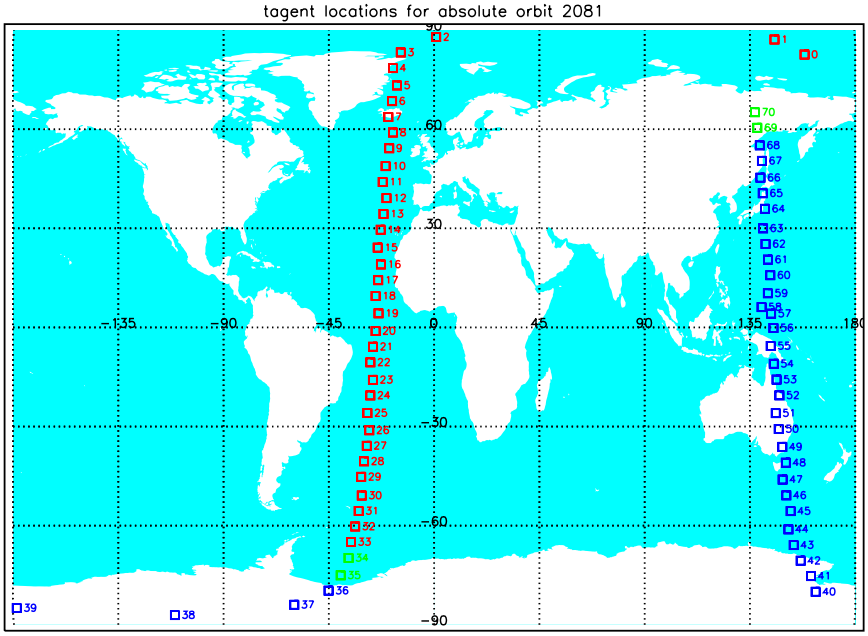

Figure 2: Tangent height geolocations for the scans of orbit #2081 taken on 24 July 2002. The numbers correspond to the scans and are used as the x-axis in the following figures. Red numbers correspond to daytime conditions and blue to nighttime. In green are for twilight.

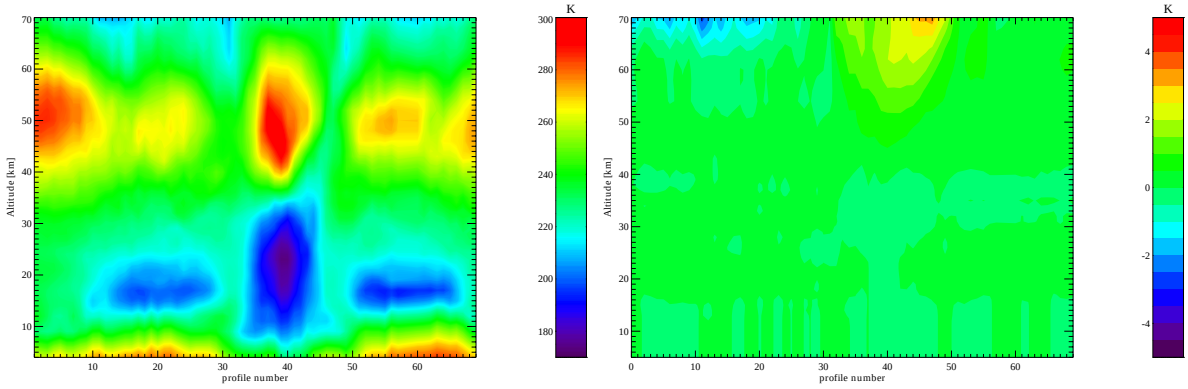

Figure 3: NLTE kinetic temperatures (left) and NLTE–LTE temperature differences (right) for orbit #2081.

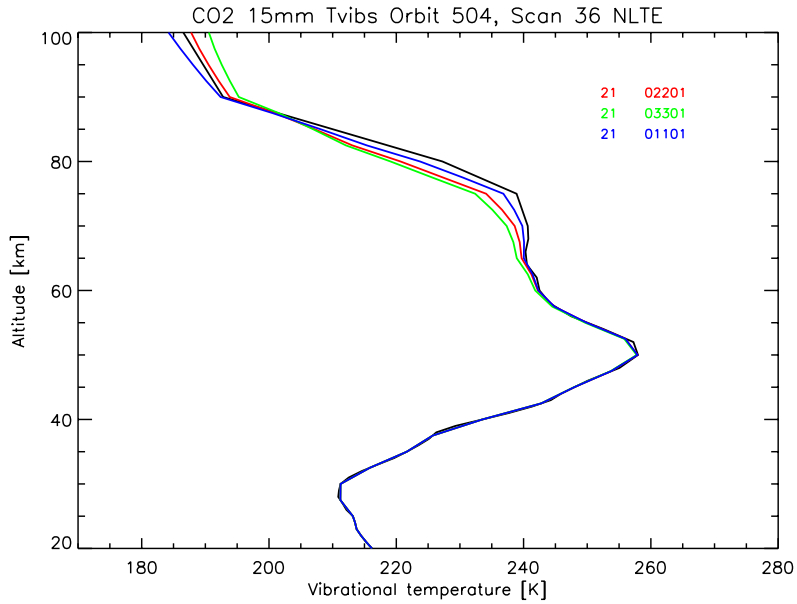

Figure 4: Vibrational temperatures for the CO_2 levels emitting the strongest emissions near 15 μm (scan 36 orbit 504).

2.2 NLTE retrievals

In the NLTE retrievals performed here, the NLTE populations, eg. the vibrational temperatures, were computed for the actual pressure-temperature and species abundances retrieved directly from the spectra. Hence, this method is more adequate and comprehensive for assessing the NLTE effects that to analyse the residuals. The NLTE retrievals were carried out for the major operational products, e.g., p-T, ozone, water vapour, methane and NO_2. In these retrievals (except for NO_2) the current information (e.g., prior to MIPAS measurements) was included. In case of NO_2, the NLTE parameters retrieved from MIPAS spectra (carried out under another project), were included here.

NLTE retrievals have been performed for orbit 2081 (see Fig. 2) for temperature-LOS (line of sight) and for O_3, H_2O, CH_4, and NO_2 volume mixing ratios (vmr). The retrievals were performed with the jointly developed IMK–IAA NLTE processor [Funke et al., 2002; Clarmann et al., 2003; Stiller et al., 2003] for the microwindows and occupation matrices used in the operational L2 processing (the so-called ESA microwindows). These are the same as those used by the IFAC processors and very similar to those of the other groups. The NLTE processor uses a forward model (KOPRA) with a generic NLTE model that calculates on-line the NLTE populations of the species at work in each iteration for the retrieved temperature profile. We should note that we do not retrieve simultaneously NLTE information but use that currently known from all previous experiments and reported in the literature. One exception is the NLTE chemical excitation of the $NO_2(v_3)$ levels, which has been retrieved from MIPAS spectra.

The results for the combined retrieval of temperature and line of sight (altitude registration) are shown in Fig. 3. The left panel shows the temperature retrieved under NLTE conditions and the right panel the NLTE–LTE differences. The NLTE model for CO_2 implemented here uses the fast collisional rate of $CO_2(v_2)$ by atomic oxygen, opposite to the moderate value used in the NLTE climatology (López-Puertas et al., 2002). The results show that NLTE induces kinetic temperature (T_k) differences smaller than $\pm$1K below $\sim$60 km. The NLTE temperatures are cooler than those retrieved under LTE in $\sim$1–2 K for daytime around 70 km. On the contrary, NLTE T_k's are warmer in 3–7 K for the polar night (scans $\sim$35–45). These results are in agreement with expectations. The cooler NLTE temperatures in the daytime are due to the larger NLTE populations obtained after the relaxation of solar absorption at 4.3 and 2.7 μm. The warmer temperatures in the polar night mesosphere result from the under-LTE populations of the $CO_2(v_2)$ levels (see Fig. 4) that occur for this warm region (see left panel of Fig. 3).

The effects of NLTE on the retrieved O_3 are shown in Fig. 5. The NLTE–LTE differences in O_3 vmr are very small ($<$2–3%) below $\sim$50 km. The retrieved O_3 under NLTE between 50–60 km is significantly smaller ($-$10%) at daytime and is larger (5–10%) in the warmer polar winter. The latter effect is caused by the underpopulation of the O_3 v_3 levels in the warm lower mesosphere, an effect similar to that shown by CO_2 in Fig. 4. The lower NLTE O_3 vmr in the daytime side is not caused by a direct local NLTE effect but by the propagation in the retrieval of

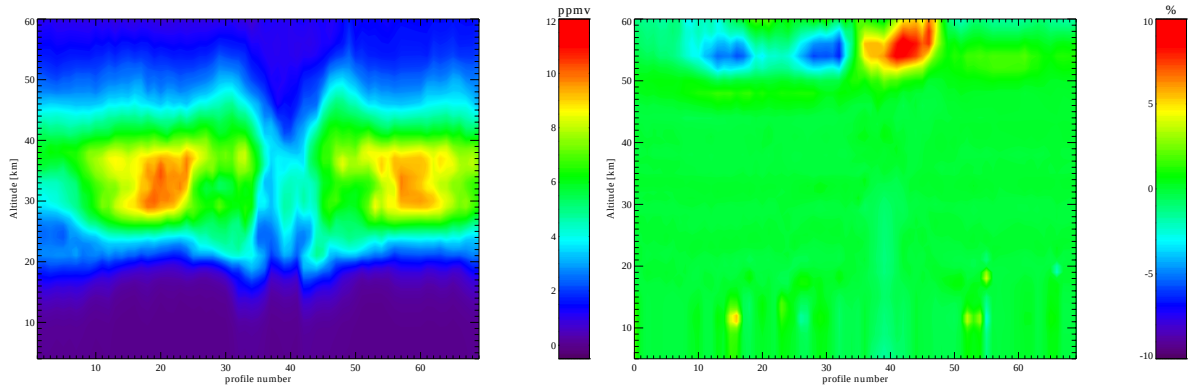

Figure 5: NLTE O_3 vmr (left) and NLTE–LTE O_3 vmr differences for orbit #2081.

the lower O_3 vmr retrieved at higher altitudes under NLTE.

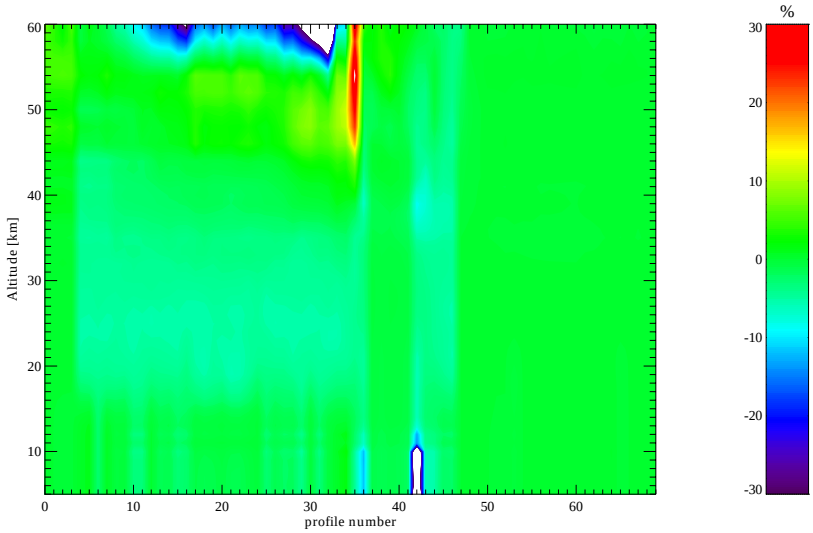

Figure 6: NLTE–LTE differences in the retrieved H_2O vmr for orbit #2081.

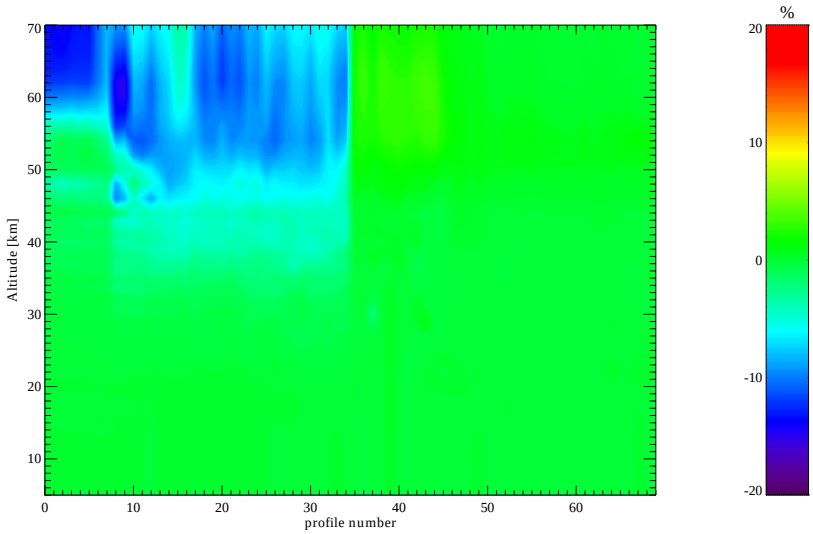

Figure 7: NLTE–LTE differences in the retrieved CH_4 vmr for orbit #2081.

The results of the H_2O vmr NLTE retrievals are shown in Fig. 6. The NLTE–LTE differences in the retrieved H_2O vmr are negligible in the whole altitude interval at nighttime. At daytime, there are significant differences

above about 55 km, reaching differences of ∼30% at 60 km, with smaller NLTE values, and also, in the 20–35 km region with differences of about –10%. The differences at heights above 55 km are due to the larger NLTE populations of the $H_2O(010)$ level in the daytime. Those at lower heights (20–35 km) are not due to local NLTE populations but induced in the retrieval method by the smaller H_2O NLTE vmr values above 55 km. The retrieved NLTE H_2O vmr can, on the other hand, be larger than in LTE (∼20%) in the lower mesosphere under polar winter conditions; when the lower mesosphere is rather warm.

The results of the CH_4 vmr NLTE retrievals are shown in Fig. 7. The NLTE effects are negligible at nighttime. At daytime, however, the theoretical NLTE model predicts smaller CH_4 vmr in about 10–15% above about 50 km. These effects might be even larger, as suggested by the residual analysis (Section 2.1). Further work on the analysis of NLTE in CH_4 using the upper atmospheric data is needed since, as shown in the day/night differences spectra (see Section 4) are larger than predicted.

NLTE effects in NO_2 were predicted to be significantly large. NLTE evidences from previous experiments were unclear or contradictory. For this reason we first attend to retrieve NLTE information from the MIPAS spectra themselves. Such work has been carried out in a different study and the main conclusion is that the chemical excitation is much smaller, by about a factor 10, than that predicted and previously assumed in the NLTE climatology (López-Puertas et al., 2002).

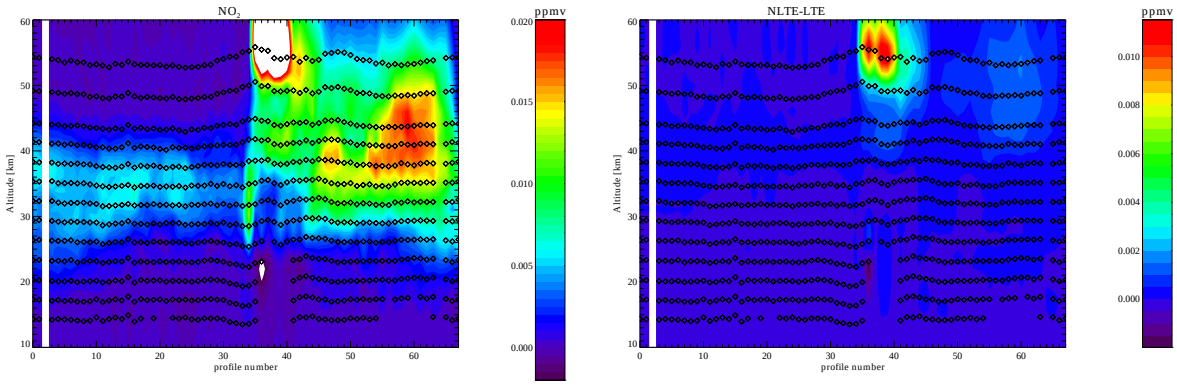

Figure 8: NLTE NO_2 vmr (left) and NLTE–LTE NO_2 vmr differences (right) for orbit #2081.

Including this new chemical excitation rate in the NO_2 NLTE model, we performed retrievals of NO_2 under NLTE. The results are shown in Fig. 8. The left panel shows the NLTE NO_2 vmr retrieved values and the right panel the NLTE–LTE differences. The resulting NLTE effects are very small (<5%) everywhere except above 50 km under polar winter conditions they can reach values close to 50%. These NLTE effects have the same origin as those mentioned above for the temperature and O_3, i.e., they are caused by radiation, and not by chemical excitation. In summary, we conclude that NLTE effects in NO_2 is, in general, very small, except for the lower mesosphere when it is very warm.

The conclusions about this workpackage can be summarised as follows:

(a) NLTE retrievals for temperature, O_3, H_2O and CH_4 for orbit #2081 show that NLTE errors are small below about 50 km. There can be however, significant errors (underpredictions) for considering LTE in the retrievals of temperature for polar-winter like atmospheric conditions (cold stratopause and warm lower mesosphere) above about 50 km.

(b) The NLTE retrievals in O_3 show that NLTE effects are small (≤5%) below 50 km but can be significant (5–15%) between 50 and 60 km, particularly in the daytime and polar winter conditions.

(c) The NLTE retrievals for H_2O show that NLTE is negligible below about 55 km, but can be significant above, in the daytime and polar winter conditions, reaching differences of up to –30% at 60 km. They can also induce differences of about –10% at 20-35 km at daytime.

(d) NLTE in CH_4 is negligible except above 50 km at daytime, where they can induce errors of about –15%. The residual analysis and the upper atmosphere measurements suggest that they might be even larger.

(e) The NLTE chemical excitation rate of NO_2 seems to be significantly smaller than predicted (at least a factor of 10 smaller). NLTE retrievals in NO_2 show that NLTE effects are small (≤5%) below ∼50 km but can be large (50%) between 50 and 60 km when we have a warm lower mesosphere, e.g., at polar winter conditions.

(f) NLTE effects are sometimes linked with the *a priori* profiles and the number of measurements (altitudes) included in the retrieval. Care should be taken to distinguish direct NLTE effects from those induced by using different *a priori* profiles and the number of measurements (altitudes) included in the retrieval.

3 WP 5512: Effects of NLTE on MIPAS retrieved species: Comparison with GOMOS and SCIAMACHY

In this workpackage we compare NO_2 and O_3 MIPAS vmr's retrieved under LTE and NLTE with the collocated measurements taken by the "NLTE free" instruments GOMOS and SCIAMACHY. The aim was to assess if potential discrepancies between LTE retrieved and GOMOS and SCIAMACHY data retrievals could be explained by the NLTE retrieved MIPAS data. A detailed description of the comparison for O_3 and NO_2 between MIPAS and GOMOS is given ion deliverable D70 (Kyrölä et al., 2003); and between SCIAMACHY and MIPAS in deliverables D64, D66, D67, D69, D71, and D72 (Milz et al., 2003). We present here some typical examples and discuss the discrepancies in terms of NLTE effects.

A detailed comparison between O_3 and NO_2 from GOMOS and MIPAS, including many figures, can be found in deliverable D70. The comparison for O_3 profiles measured near-collocated shows a reasonable agreement. Also the statistical comparison with relaxed collocation shows a promising agreement. The differences found between the measurements of both instruments cannot be explained by NLTE since they mostly occur at low altitudes where NLTE effects are negligible. The comparison for NO_2 profiles is difficult because of large oscillations in GOMOS profiles. This causes differences much larger than what one would expect from NLTE even in the most pessimistic cases.

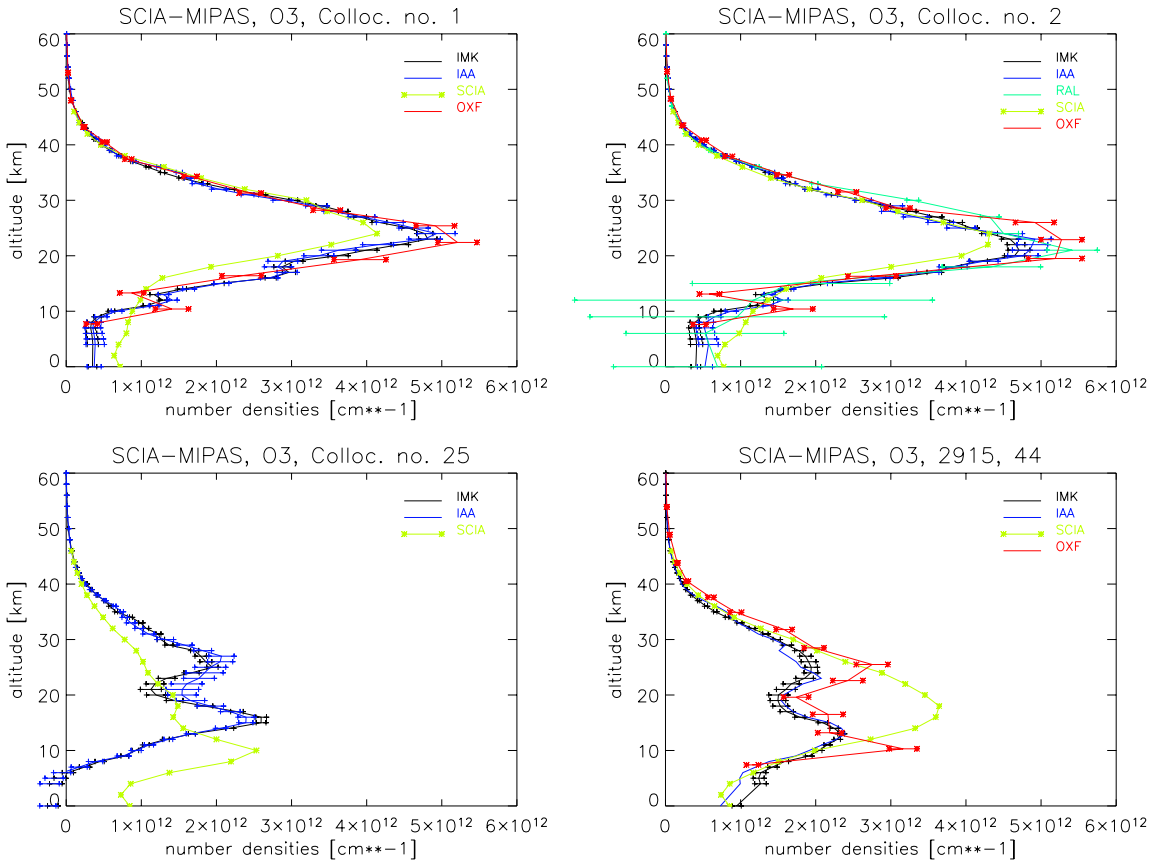

Figure 9: Comparison of O_3 number density profiles measured by MIPAS and SCIAMACHY on 20 and 23 Sept. 2002. For details on the geolocations see Table 1 in Milz et al. (2003). The two figures in the upper panel show the profiles for collocations outside the polar vortex; the two at the bottom, inside the polar vortex. Results from UB-SCIA (SCIA, yellow), IMK (MIPAS-LTE, black), IAA (MIPAS-NLTE, blue), OXF (MIPAS-LTE, red), and RAL (MIPAS-LTE, green). Horizontal bars in MIPAS retrievals represent random errors.

Figure 9 shows four typical comparisons for collocations between MIPAS and SCIAMACHY measurements for O_3. The two at the top are for collocations outside the vortex and the two at the bottom for collocations inside the vortex. The details of the measurements, collocations, datasets, etc. can be found in Milz et al. (2003). Ozone has been retrieved from MIPAS by three processors: IMK and Oxford (OXF) under LTE and IAA under NLTE. The latter is an extension of the IMK code but including NLTE. In general, the differences between the three retrievals of MIPAS O_3 are much smaller than between any of these with the O_3 retrieved from SCIAMACHY. The SCIAMACHY O_3 is generally smaller than the MIPAS retrievals and seems to show less vertical resolution. It is particularly interesting to note that the IMK-IAA differences, which are a good indication of the NLTE effects, are much smaller than any of these with SCIAMACHY results (see, e.g., the bottom panels in Fig. 9). The conclusion then is that, at least with the current state of SCIAMACHY O_3 retrievals, the differences between MIPAS and SCIAMACHY O_3 are much larger than would be expected from NLTE effects and these, if of any significantly, are much smaller than current differences. For other possible explanation of these differences see Milz et al. (2003).

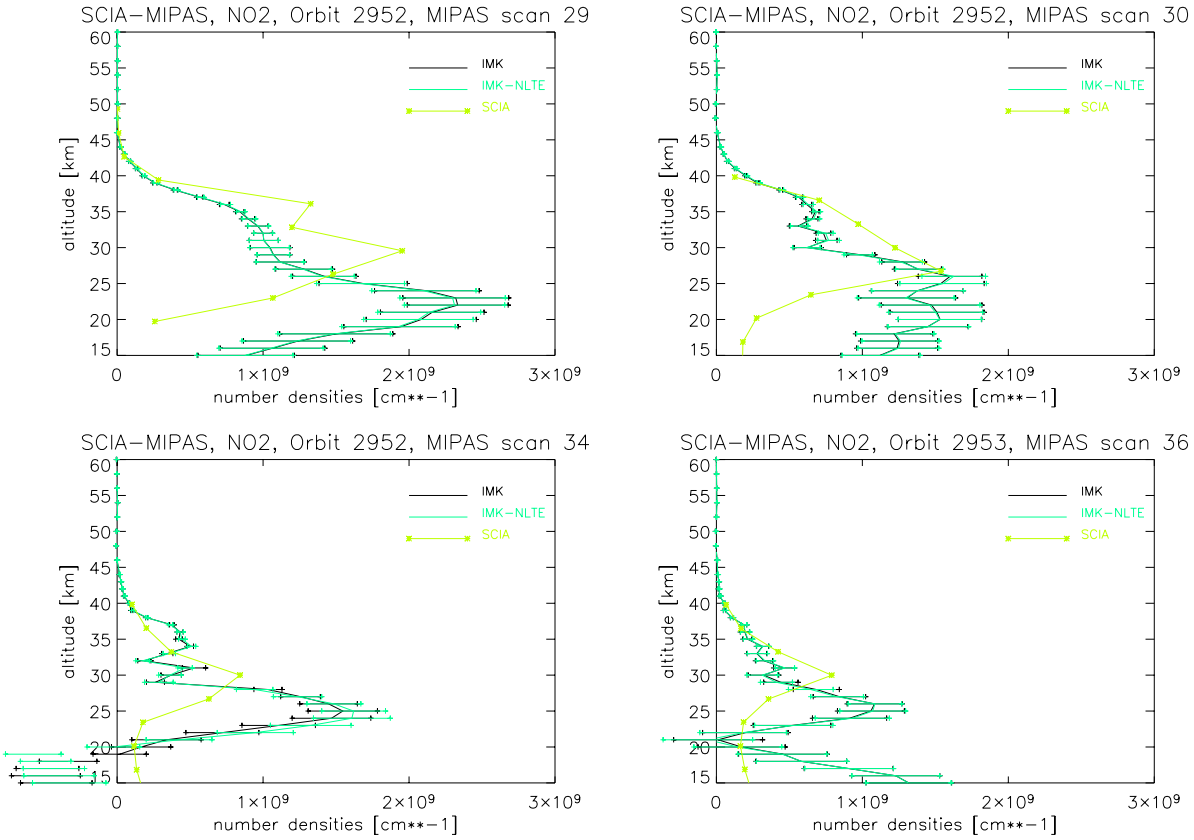

Figure 10: Comparison of NO_2 number density profiles measured by MIPAS and SCIAMACHY on 23 Sept. 2002. For details on the geolocations see Table 2 in Milz et al. (2003). Results from UB-SCIA (SCIA, yellow), IMK (MIPAS-LTE, black), and IMK-NLTE (MIPAS-NLTE, green). Horizontal bars in MIPAS retrievals represent random errors.

Figure 10 shows the comparison between SCIAMACHY and MIPAS for NO_2 for six collocations. MIPAS NO_2 have been retrieved under LTE and NLTE conditions with the IMK and IMK/IAA processors. As for O_3, we see that the differences induced by NLTE (IMK-NLTE) and IMK-LTE are much smaller than the differences between either NLTE or LTE retrievals with the SCIAMACHY measurements. It is then clear that NLTE effects cannot explained the observed MIPAS/SCIAMACHY differences.

4 WP 5513: Characterisation of NLTE effects in terms of day/night differences in MIPAS spectra

Another aspect of the NLTE study was to analyse NLTE effects in the actual MIPAS spectra. For that, a comparison between co-added spectra at daytime and nighttime was undertaken for orbits #504 and 2081 (nominal mode) and for those taken in MIPAS upper atmosphere mode (#1748-1752). NLTE were analysed for most of the bands of the atmospheric species, including CO_2, O_3, H_2O, CH_4, NO_2, NO, CO and OH.

The spectra were co-added for day and night conditions in order to minimize the noise and enhance potential NLTE emissions. In some cases the day/night temperature variability avoid from identifying small NLTE effects. Also, for those species which exhibit a large diurnal variation (e.g., O_3 and NO_2) it is difficult by this analysis to discern NLTE effects from actual vmr changes.

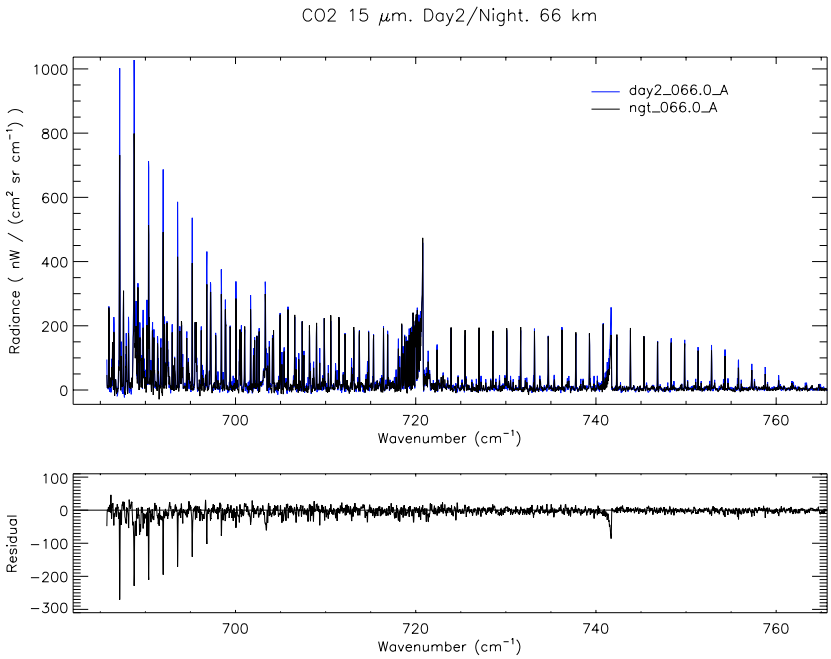

Figure 11: CO_2 day/night MIPAS spectra in the 15 μm region (band A).

Figure 11 shows the day and night co-added spectra for orbit 504, at a tangent height of 66 km in MIPAS band A. The number of co-added spectra for the daytime case is of 7 and of 12 for the case of nighttime. The noise in this spectra is significantly smaller than in single spectra. In the lower panel of the figure we show the Night–Day spectra (in absolute units). This shows significant differences, with larger values in the daytime. There are some experimental evidence (López-Puertas and Taylor, 2001) that the CO_2 15 μm bands, particularly the hot bands are enhanced in the daytime. The differences shown here are in consonance with that prediction but it could well be that what we are observing for this particular case is a larger mesospheric temperature in the nighttime than in the daytime. In addition to this, we have taken the 5 orbits measurements taken in the MIPAS upper atmosphere mode on 1st July 2002 (orbits 1748–1752) and have calculated the daytime enhancement ((day-night)/night) in the spectra integrated over the CO_2 15 μm region (685–800 cm^{-1}) for a range of latitudes from 50°S to 50°N (see Fig. 12). The figure shows that with the exception of some latitudes (equator) at 90–100 km, there is a general daytime enhancement in the radiance above around 70 km, reaching values larger than 100% around 90 km. This enhancement is in consonance with our expectations and hence should not affect the retrieval of temperature of the different processors. Note the enhancement is above 70–75 km, while the retrieved temperature stop at 68 km.

Figure 13 shows a similar day/night spectra for the band AB of MIPAS. Tangent height is of 68 km. The lower panel show in this case the day–night spectra. We can appreciated two distinct features. We see a daytime enhancement in the CO_2 laser bands centred near 1060 cm^{-1}, as it is expected, due to solar pumping of the CO_2(001) levels in the daytime. We also appreciated a nighttime enhancement in the region of the O_3 (001→000) band, as a consequence of the larger mesospheric O_3 abundance at nighttime. We can also see this nighttime enhancement, although smaller, in the O_3(100→000) band in the upper panel around 1120 cm^{-1}.

Figure 14 shows a day/night MIPAS spectra in band B at a tangent height of 66 km for orbit 1748. This

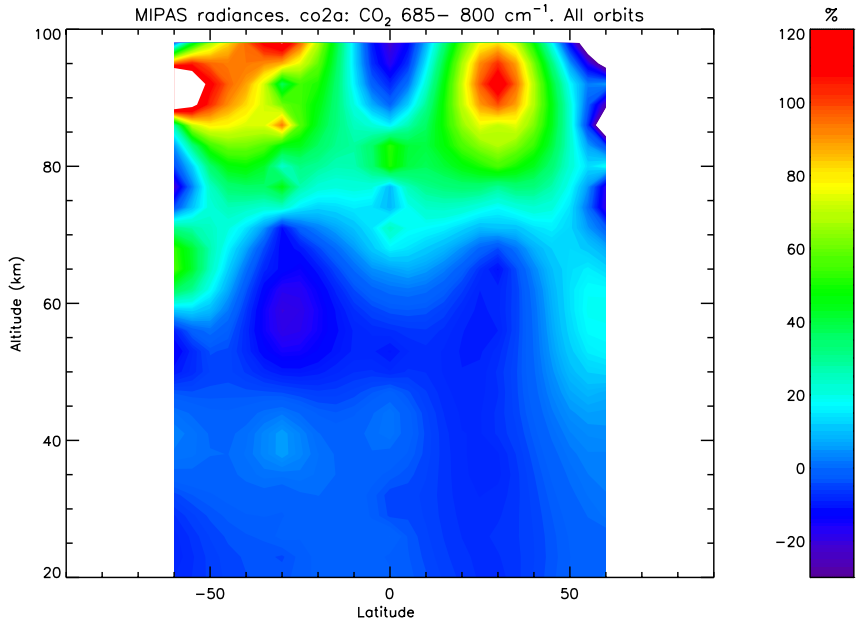

Figure 12: Daytime enhanced radiances [(Day–Night)/Night] in the CO_2 15 μm spectral region for the 5 upper atmospheric orbits taken on July 1 2002.

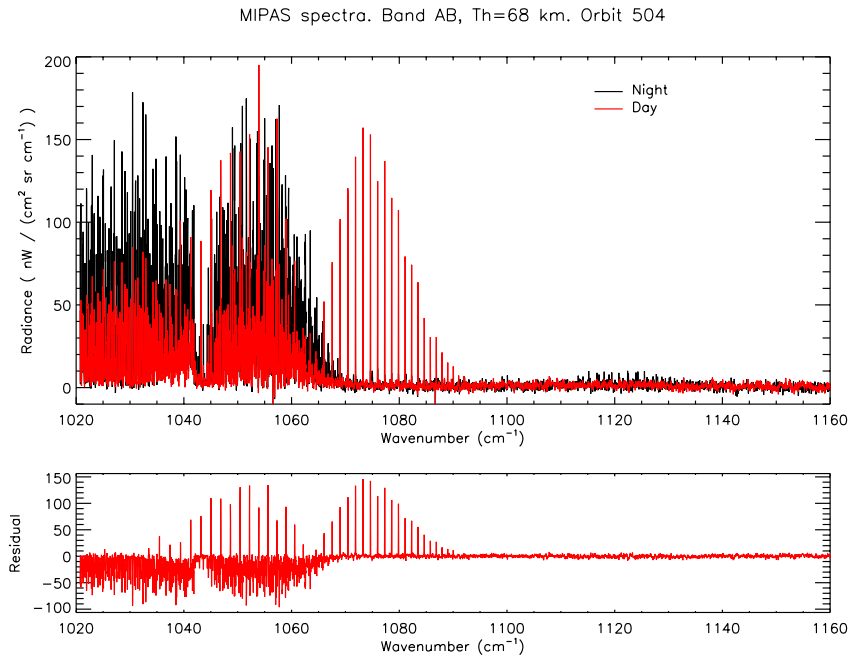

Figure 13: Day and night MIPAS spectra in the 10 μm region (band AB).

spectral region is dominated by CH_4 and H_2O lines. The day–night difference spectra (lower panel) also show clear features of daytime enhancement in many lines. Figure 15 shows in a larger scale the spectra where it is clearly appreciated that the spectra for the two daytime latitude bands are larger than the nighttime spectra. The stronger lines in this figure corresponds to the CH_4 υ_2 lines. Since CH_4 is well mixed in the mesosphere and its chemical lifetime is very long, we do not expect this to be due to a diurnal change in CH_4 abundance. Daytime temperatures for the case day2 (covering latitudes from the North pole to 30°S) might be larger than nighttime (Fig. 11) but in case day1 (covering latitudes from the northern tropic to 60°S), the temperature was lower than in nighttime and, even though, we find a larger CH_4 emission in day1 than in night. It is highly possible that this daytime enhancement is a NLTE feature caused by solar pumping in CH_4 bands. These measurements thus constitutes the first experimental evidence of CH_4 NLTE emission in the atmosphere.

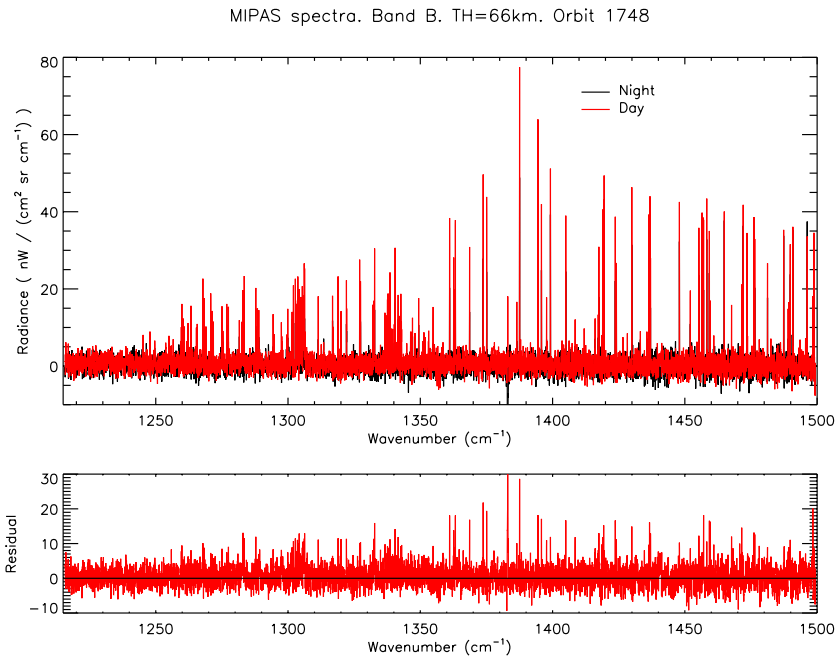

Figure 14: Day and night MIPAS spectra in band B.

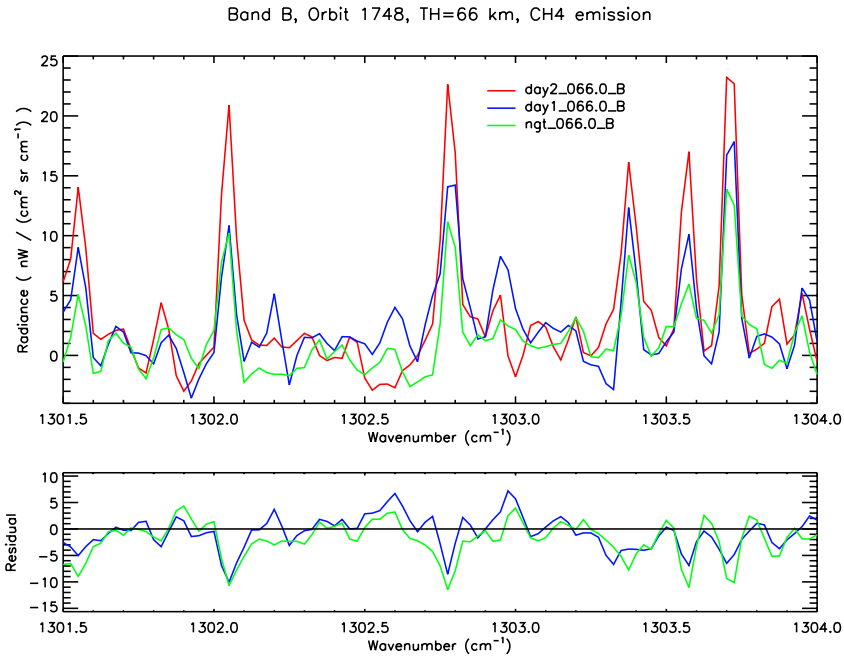

Figure 15: Day and night MIPAS spectra in band B showing CH_4 lines.

We also carried out a similar analysis as before for CO_2 15 μm. We computed the day/night difference for the 5 orbits on 1st July for the 50°S–50°N latitude band (see Figure 16) integrating the radiance in the 1215–1350 cm^{-1} spectral interval, dominated by CH_4 bands. Again we found a systematic daytime enhancement for the most latitudes, starting roughly around 55–60 km. This is qualitative consistent with our prediction but the magnitude of the deviation from LTE seems to be underestimated by a factor of 2. Hence, NLTE effects in the CH_4 retrievals, as shown in Section 2.2, seems to be underestimated.

A similar study has been carried out for H_2O in band C of MIPAS. Figure 17 shows the day and night spectra in MIPAS band C for a tangent height of 68 km, orbit 504. It also shows in the lower panel, day–night difference spectra, significant features clearly enhanced in the daytime. A closer look at the spectra (Fig. 18) shows that

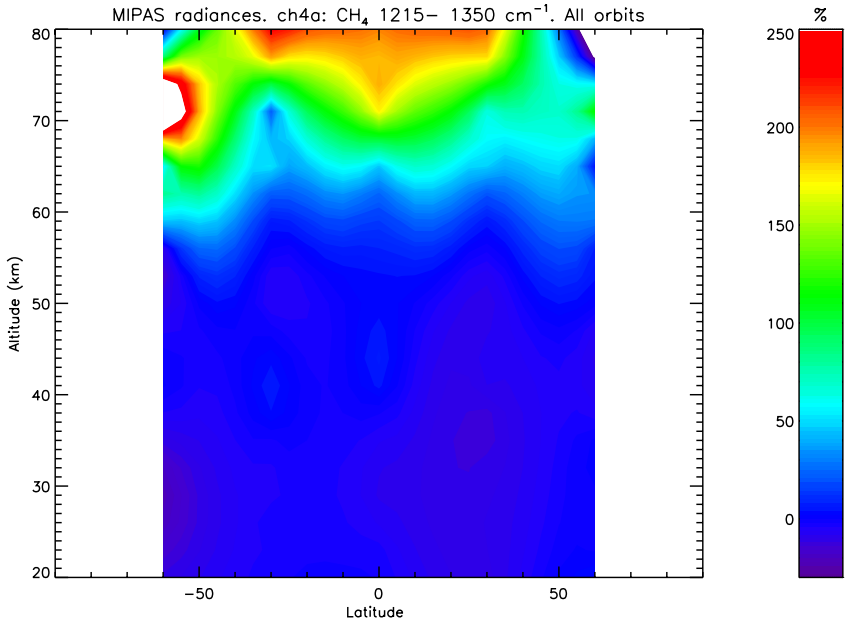

Figure 16: Daytime enhanced radiances [(Day–Night)/Night] in the CH_4 spectral region for the 5 upper atmospheric orbits taken on July 1 2002.

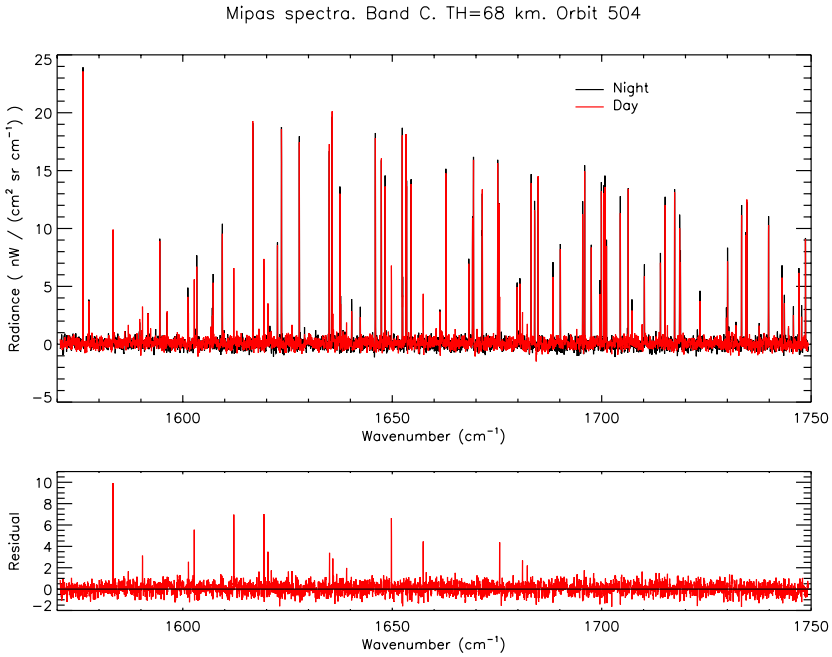

Figure 17: Day and night MIPAS spectra in band C showing H_2O lines.

the enhanced lines correspond to the $H_2O(020\rightarrow010)$ first hot bands lines. These lines have been identified in the past ISAMS, CRISTA and CIRRIS measurements but never with such a clear and nitid distinction from the fundamental lines contribution. Preliminary calculations show that they are of similar magnitude than the predicted NLTE emission.

As have been done with CO_2 15 μm and CH_4 bands, we also computed the daytime enhancement as a function of latitude for the upper atmosphere orbits (see Fig. 19). The spectra were integrated over the 1300–1630 cm^{-1}. The measurements show also a clear daytime enhancement for most latitudes above about 60 km.

The analysis of the day/night MIPAS spectra has also revealed the existence of many other NLTE emissions in the atmosphere. Fig. 20, for example, shows the emission form the first hot band (2→1) of nitric oxide (NO). The strong line in the middle is the fundamental NO(1→0) band, while the two smaller peaks at each side correspond

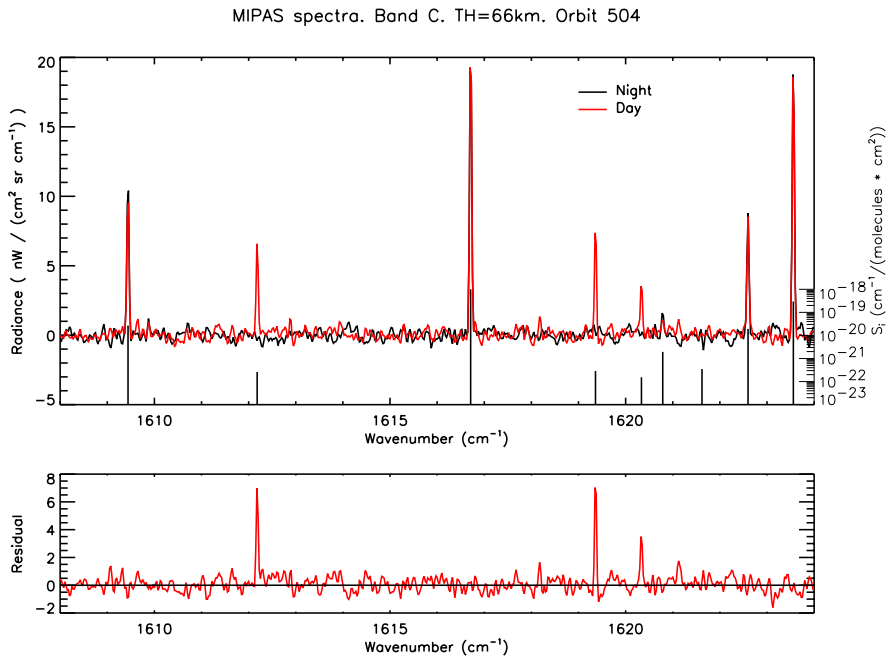

Figure 18: Day and night MIPAS spectra in band C showing H_2O first hot band lines.

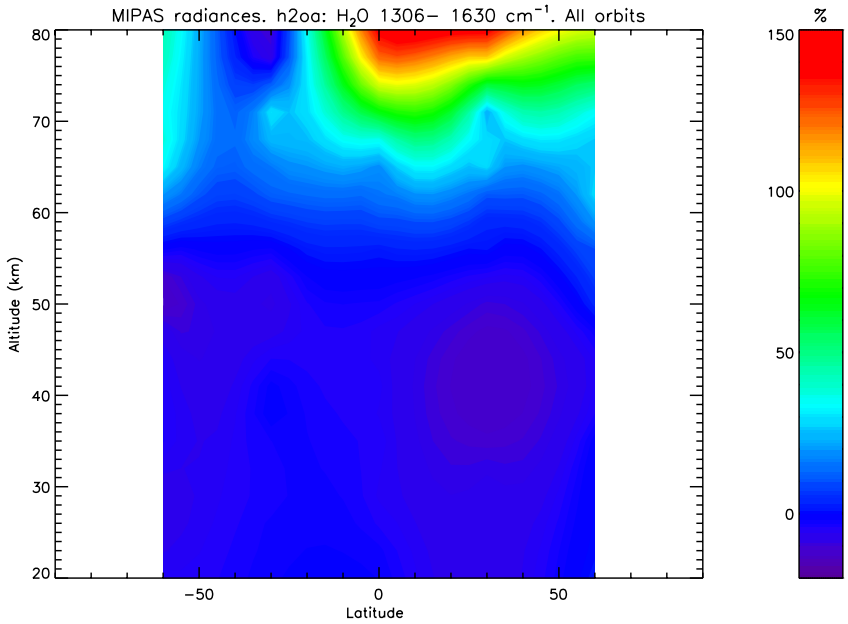

Figure 19: Daytime enhanced radiances [(Day–Night)/(Day+Night)] in the H_2O spectral region for the 5 upper atmospheric orbits taken on July 1 2002.

to the emission of several lines (in each peak) of the NO(2→1) band. This has been occasionally measured under perturbed atmospheric conditions at high altitudes but here we see under quiet conditions and at low altitudes.

Figure 21 shows the day and night spectra for orbit 1748 at a tangent height of 56 km in the region of 2029.5 cm^{-1}. The spectra show a clear daytime enhancement. The contributing lines in this region have been identified as from the O_3 (102→001) combination band. Since O_3 has a larger concentration at nighttime, this daytime enhancement clearly reflect a much larger NLTE population of the O_3(102) level relative to LTE in the daytime. This provides an unique information for understanding the NLTE populations of O_3 vibrational levels.

Figure 22 shows the day and nighttime spectra for orbit 1750 at a tangent height of 71 km in the region around 2100 cm^{-1}. The two most prominent features are two lines of the fundamental CO (1→0) band. The three weaker lines, which disappear in the nighttime spectrum, have been identified as due to the CO first hot band. To our

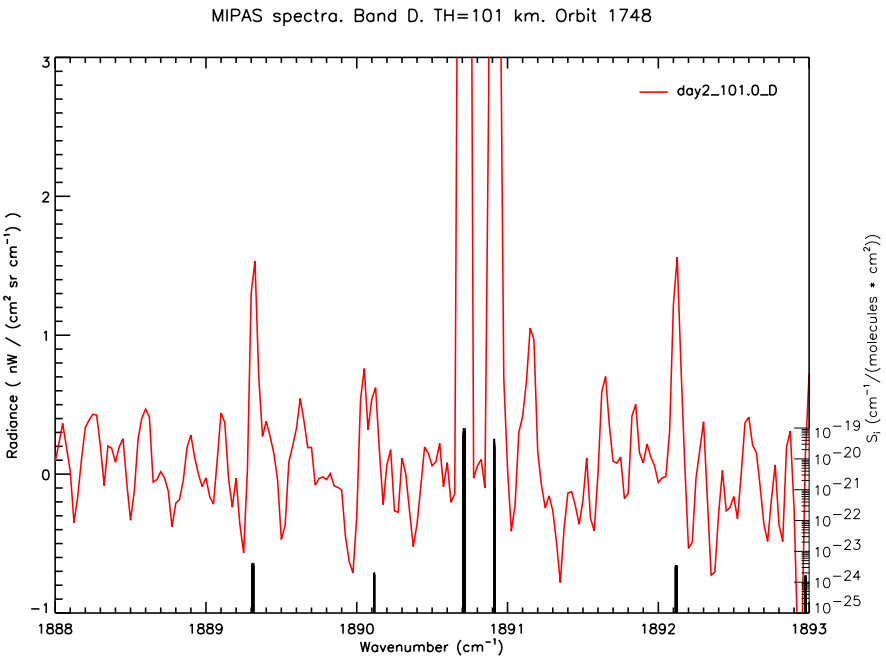

Figure 20: Daytime MIPAS spectra in band D showing NO fundamental and first hot lines.

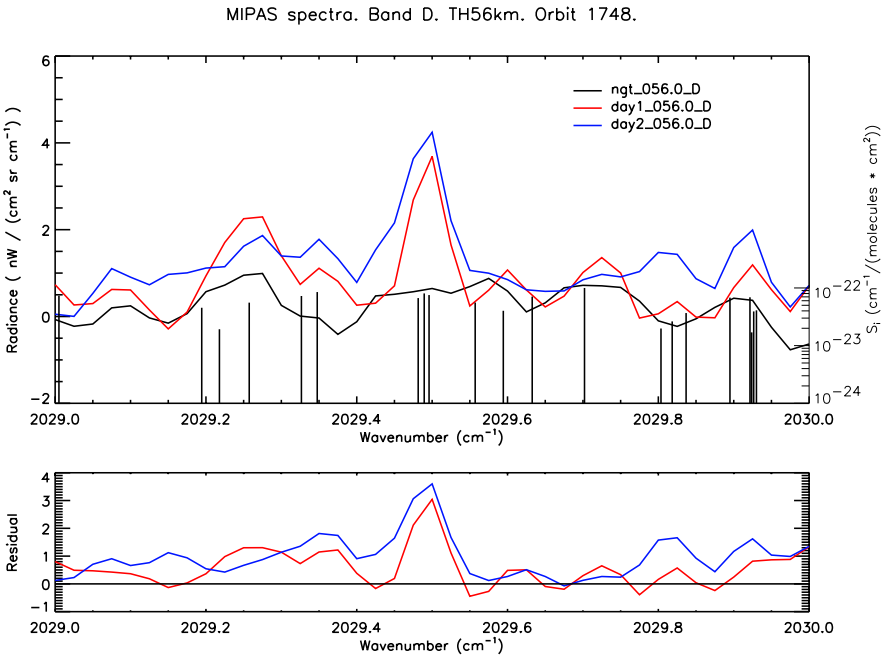

Figure 21: Day and night MIPAS spectra in band D showing O_3 lines of the (102→001) combination band.

knowledge it is the first time that these lines have been measured in the atmosphere. This is important *per se* and would also help for understanding the NLTE of CO in the 4.6 μm region and might be useful also for improving the retrieval of CO at stratospheric tangent heights in the daytime.

Figure 23 shows the nighttime co-added spectra for orbit 1750 at tangent heights of 76, 81 and 86 km in the region around 2238 cm^{-1}. This shows how MIPAS, although weakly, is also sensitive to the mesospheric OH Meinel bands. In particular the emission in the centre of the figure has been identified as due to a Q-branchline of the OH(9→8) band. This then shows that upper atmosphere MIPAS spectra also provides information about the population of OH(9) in the nighttime mesosphere.

In summary, the analysis of NLTE in the day/night spectra show, in general, the major expected NLTE features.

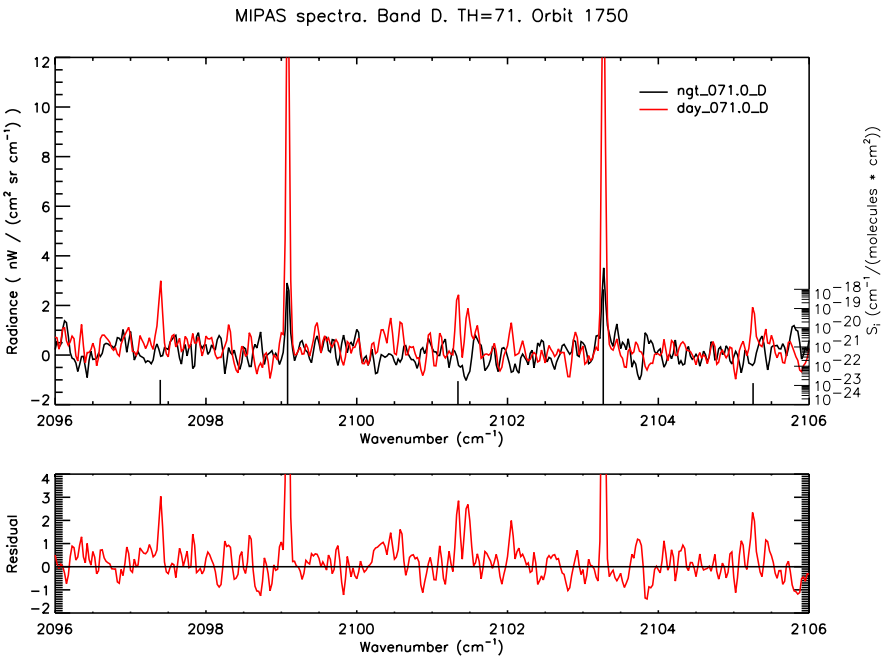

Figure 22: Day and night MIPAS spectra in band D showing CO lines of the fundamental and first hot bands.

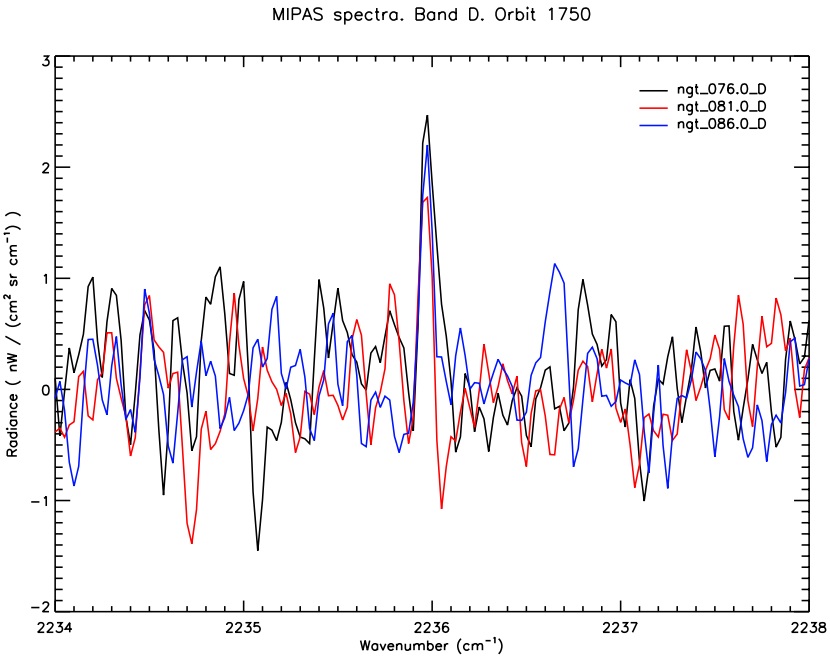

Figure 23: Nighttime MIPAS spectra in band D at different tangent heights showing the contribution of the OH (9→8) band.

Exceptions are NO_2, for which the NLTE effects seem to be significantly smaller than predicted, and CH_4, for which NLTE seems to be larger than theoretically predicted. The latter needs a detailed analysis for an accurate assessment.

Furthermore, this analysis have also revealed the existence of many first detected NLTE emissions, as well as more clear and nitid determinations of some previously detected NLTE features. These new detected emissions, however, do not affect the retrievals of most species, since they are located out of the microwindows normally used for the species retrievals.

5 References

Clarmann, v.T., T.C. Chineke, H. Fischer, B. Funke, M. García-Comas, S. Gil-López, N. Glatthor, U. Grabowski, M. Höpfner, S. Kellman, M. Kiefer, A. Linden, M. López-Puertas, G. Mengistu-Tsidu, M. Milz, T. Steck, and G.P. Stiller, Remote sensing of the middle atmosphere with MIPAS, *Remote Sensing of Clouds and the Atmosphere VII*, K. Schäfer, O. Lado-Bordowsky, A. Comeron (eds.), *Proc. SPIE*, **4882**, 172–183, 2003.

Dudhia, A. et al., MIPAS microwindows selection and error budget, *Proc. Envisat Validation Worshop*, ESA SP-531, ESA SP-531, Noordwijk, 2003.

Funke, B., M. López-Puertas, G. Stiller, T. von Clarmann, and F. J. Martín-Torres, New non-LTE retrieval method for atmospheric parameters from MIPAS/ENVISAT emission spectra at 5.7 μm, *Remote Sensing of Clouds and the Atmosphere VI*, K. Schäfer, O. Lado-Bordowsky, A. Comeron, M.R. Carleer and J.S. Fender (eds.), *Proc. SPIE*, **4539**, 396-405, 2002.

Kyrölä, E., J. Tamminen, and V. Sofieva, GOMOS-MIPAS comparison, D70, 2003.

López-Puertas, M., et al. Advanced MIPAS Level 2 Data Analysis (AMIL2DA), Project EVG1-CT-1999-00015, Report on the Climatology of Vibrational Temperatures, March 2002.

López-Puertas, M. and F. W. Taylor, *Non-LTE Radiative Transfer in the Atmosphere*, World Scientific Publishing Co., Singapore, 2001.

Milz et al., Comparison of AMIL2DA results for MIPAS-ENVISAT data with external data (D64, D66, D67, D69, D71, D72), 2003.

Stiller, G.P., v.T. Clarmann, T.C. Chineke, H. Fischer, B. Funke, S. Gil-López, N. Glatthor, U. Grabowski, M. Höpfner, S. Kellman, M. Kiefer, A. Linden, M. López-Puertas, G. Mengistu-Tsidu, M. Milz, and T. Steck, Early IMK/IAA MIPAS/Envisat results, *Remote Sensing of Clouds and the Atmosphere VII*, K. Schäfer, O. Lado-Bordowsky, A. Comeron (eds.), *Proc. SPIE*, **4882**, 184–193, 2003.